PHYSICAL REVIEW B

CONDENSED MATTER

THIRD SERIES, VOLUME 42, NUMBER 2 15 JULY 1990-I

Measurement of the partial photoionization cross section and the asymmetry parameter of the Ag valence band near the 4*d* threshold

M. Ardehali and I. Lindau

Stanford Electronics Laboratories, Stanford University, Stanford, California 94305

(Received 15 May 1989; revised manuscript received 2 April 1990)

Measurements of the partial photoionization cross section (σ) and of the photoelectron asymmetry parameter (β) have been performed on polycrystalline Ag around the 4*d* threshold. A description of the technique used to obtain σ and β from the photoemission spectra is provided. It is shown that in the condensed phase, the photoelectron asymmetry parameter can be experimentally determined much more accurately than the partial cross section, because many experimental uncertainties, such as the dependence of the intensity of the light source with the photon energy, the variation of the electron mean free path, and the transmission and counting efficiency of the electron analyzer as a function of the kinetic energy of the photoelectron, which introduce a considerable amount of distortion in the measurements of σ, do not play a role in determining β. Near the threshold, the σ from bulk Ag is very close to the atomic results, whereas the β is severely distorted with respect to the free atom, being essentially equal to zero. We propose that the isotropy of the photoelectron angular distribution in polycrystalline Ag is primarily a consequence of a double randomization by a diffraction process of the final states due to the crystal potential and by random orientation of the crystallites. We also point out that there is an interesting analogy between the results of our photoemission experiment and the "Debye-Scherrer pattern" of an x-ray-diffraction experiment from a powder of crystals oriented at random.

I. INTRODUCTION

In a photoemission experiment, the energy of the incoming photon flux absorbed in solid or gas is converted principally into the kinetic energy of the electrons, with the intensity and the angular distribution of the photoelectrons providing information about the initial and the final states responsible for the absorption. In experiments in which the photoelectrons are collected by an angle-integrated electron analyzer, for example by a cylindrical mirror analyzer (CMA), only the intensity which is proportional to the partial photoionization cross section can be measured. However, for photoelectron spectroscopy to realize its full potential, experiments must be designed in which both the intensity and the angular distribution can simultaneously be measured, thereby allowing the determination of the partial cross section and the asymmetry parameter. In the last few years, with the advances in the experimental techniques and with the advent of the synchrotron radiation as a suitable source of monochromatic light, a considerable amount of research effort has been devoted to the measurements of the photoelectron asymmetry parameter in the gas phase (both atoms and molecules) over a wide range of photon energies, giving a wealth of information about the photoexcitation dynamics, resonances, many-body effects, and the Cooper effect.[1-3] In the condensed phase, however, there have only been three studies of the photoelectron asymmetry parameter, all at energies well above the threshold.[4-6]

In this paper, we report on the first experimental determinations of the 4*d* asymmetry parameter of Ag valence band in the photon energy range $h\nu = 14-34$ eV. We will show that the β from metallic Ag is severely distorted with respect to the free atomic case, showing a much smaller energy dependence, and we suggest an interpretation scheme for such a remarkable behavior of the bulk Ag asymmetry parameter. We will also indicate that in the condensed phase, the photoelectron angular distribution of all states—either core levels or valence states—are expected to be essentially isotropic at energies near the threshold.

This paper is organized into the following sections. Section II deals with the experimental set up and the sample preparation. Section III is devoted to a detailed description of the techniques used for the measurements of the cross section and the asymmetry parameter; in this section we show that in the condensed phase, β can experimentally be determined much more accurately than σ. In Sec. IV, we present our experimental data for the cross section and the asymmetry parameter of polycrystalline Ag, and discuss their behavior near the threshold. Conclusions are summarized in Sec. V.

II. EXPERIMENTAL

The experiments reported here were conducted on the 8° beam line at Stanford Synchrotron Radiation Laboratory during the dedicated run with 3 GeV and about 50-mA beam current. Photon energies between 14 and 34 eV were used to look at the valence-band energy distribution curves of polycrystalline Ag. The intensity of the light beam was monitored by the electron yield of a sodium salicylate[7] net placed between the monochromator and the experimental chamber. The photoelectrons were collected by a movable hemispherical electrostatic analyzer (VG Scientific) operated in the constant-retarding-ratio mode ($\Delta E/E=$const) in order to take advantage of the resulting transmission function.[8] The analyzer acceptance cone, 2° in half-angle, could be freely oriented relative to the sample normal by rotating it in a cone around the sample normal. The energy band pass of the electron analyzer was set at approximately 0.25 to 0.3 eV in order to reduce the contribution of the secondary electrons to the measured photocurrent.

The polycrystalline Ag was prepared by *in situ* evaporation of almost 5000 Å of Ag onto a clean stainless-steel substrate at room temperature at a pressure of 2×10^{-10} Torr or better (base pressure 5×10^{-11} Torr). The sample was positioned at the center of the chamber, with its surface at the common focus on the analyzer and the light beam. All of the experimental cross section and the asymmetry parameter data were taken at normal incidence in order to reduce the light reflection and refraction at the sample surface.

III. EXPERIMENTAL DETERMINATION OF THE PARTIAL CROSS SECTION AND THE ASYMMETRY PARAMETER

A. Cross section

In this work, we measured the relative value of the cross section (in arbitrary units), without calibrating σ on an absolute megabarn (Mb) scale. The uncertainty connected with the absolute calibration of the experimental data is rather significant because of the lack of knowledge of the exact number of photons per cm^2 sec provided by the synchrotron light source and because of the uncertainties involved in the determination of the absolute values of some of the correction factors (such as the electron mean free path, the analyzer efficiency, and the light reflection and refraction at the sample surface).

The measuring counting rate $C(h\upsilon)$ is related to the differential cross section (in arbitrary units) by the equation

$$C(h\upsilon)\propto\frac{d\sigma(h\upsilon)}{d\Omega}\lambda(E_k)\xi(E_k)\Phi(h\upsilon)F(\lambda,\kappa,\eta,\chi)\cos\gamma\ , \tag{1}$$

where $\lambda(E_k)$ is the electron escape depth which depends on the photoelectron kinetic electron; $\xi(E_k)$ is the efficiency of the electron analyzer; $\Phi(h\upsilon)$ is the relative photon flux arriving at the sample; γ is the angle between the sample normal and the photoelectron direction, and F accounts for the light reflection and refraction at the sample surface. The function F depends on the electron escape depth λ, the complex index of refraction of the sample surface $\eta+i\kappa$, and the incident angle of the light χ. The differential cross section measured by the angle-resolved electron analyzer is related to the partial photoionization cross section by Yang's equation:[9]

$$\frac{d\sigma_{\rm nl}(\varepsilon)}{d\Omega}=\frac{\sigma_{\rm nl}(\varepsilon)}{4\pi}[1+\beta P_2(\cos\alpha)]\ , \tag{2}$$

where α is the angle between the polarization vector and the photoelectron direction and $P_2(\cos\alpha)=\frac{1}{2}(3\cos^2\alpha-1)$. The partial cross section σ was measured by setting the electron analyzer at the so called magic angle $\alpha_{\rm mag}=54.7°$, where the coefficient of the asymmetry parameter vanishes, and the differential cross section thus becomes proportional to the partial cross section, i.e., $(d\sigma/d\Omega)\alpha_{\rm mag}=\sigma/4\pi$. The energy dependence of the photoionization cross section was then simply obtained by measuring the area under the photoelectron peak as a function of the photon energy and making proper normalization for the incoming photon flux, the electron escape depth and the reflection of the light beam at the sample surface. The accuracy of our data is essentially limited by the uncertainty in the photon flux estimation, which amounts to about ±25%. However, as will be shown in Sec. II B, the uncertainty connected with the measurement of the β parameter is considerably smaller, perhaps as small as ±5%.

B. Asymmetry parameter

The measurement of the β parameter in the condensed phase is experimentally more difficult than in the gas phase (the interpretation of the data is also considerably more difficult). In the gas phase, the photoelectron asymmetry parameter can easily be obtained by taking photoemission spectra at two different ejection angles and fitting the results to the form of Eq. (2). In the condensed phase, however, as seen in Eq. (1), the measuring counting rate depends both on the angle between the sample normal **n** and the photoelectron direction **p** (through $\cos\gamma$) and on the angle between the sample normal and the direction of the incoming light [through the function $F(\chi)$]. To measure the condensed phase asymmetry parameter, it is therefore necessary to keep both γ and χ constant, while varying the angle between the polarization vector and the photoelectron direction α. This can be achieved by rotating the electron analyzer in a cone

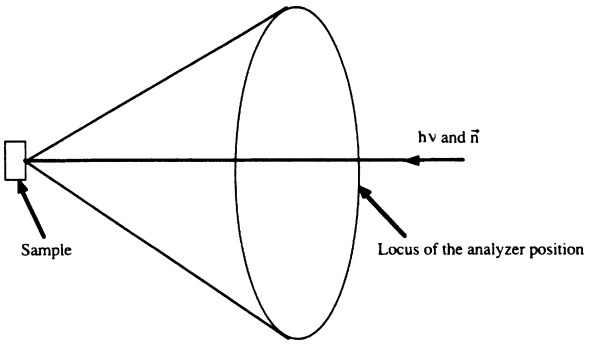

FIG. 1. Simple geometry of the experiment showing the position of the electron analyzer.

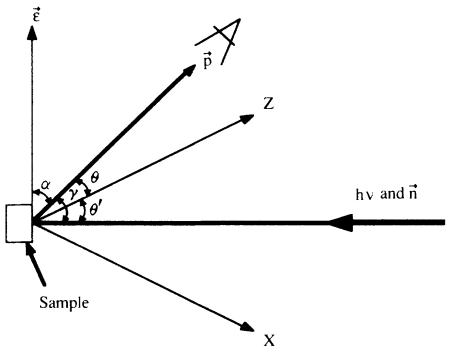

FIG. 2. Geometrical configuration of the experiment showing the various parameters.

around the sample normal.

The experimental configuration is depicted in Figs. 1 and 2. During the experiment, the incoming light was impinging on the sample surface at normal incidence, that is, the direction of the $h\nu$ was parallel to the sample normal **n**. We now define our coordinate system. We assume that the Z axis lies in the plane of incidence (i.e., in the plane of the photon direction and the polarization vector), with the plane constructed from the Z axis and the photoelectron direction being perpendicular to the plane of incidence. This requirement uniquely specifies the Z axis. We also assume that the X axis is in the plane of incidence, at 90° with respect to the Z axis, and the Y axis is perpendicular to the X-Z plane (Fig. 2).

The angle between the sample normal and the photoelectron direction (γ) in the X,Y,Z coordinates is given by

$$\cos\gamma=\cos\theta\cos\theta'+\sin\theta\sin\theta'\cos(\phi-\phi') , \tag{3}$$

where θ and θ' are the angles of **p** and **n** with respect to the Z axis, and ϕ and ϕ' are the angles of **p** and **n** with respect to the X axis. Since the photoelectron direction **p** is in the Y-Z plane, thus $\phi=90°$, and because the light direction is in the X-Z plane, hence $\phi'=0°$. Thus Eq. (3) reduces to

$$\cos\gamma=\cos\theta\cos\theta' . \tag{4}$$

For a fixed value of γ, Eq. (4) can be used to determine the position of the electron analyzer. The procedure is as follows:

(1) Choose an angle γ and keep it constant throughout the experiment. In our experiment, we fixed γ at 60°, where Eq. (4) reduces to

$$\cos\theta=\frac{1}{2\cos\theta'} . \tag{5}$$

(2) Choose an angle θ'. Rotate the electron analyzer by angle θ' in the plane of incidence.

(3) Determine θ from Eq. (5). Rotate the electron analyzer by angle θ in the plane perpendicular to the plane of incidence. Take the photoemission spectra.

(4) Determine the angle between the polarization vector $\boldsymbol{\varepsilon}$ and the photoelectron direction **p**, i.e., the angle α. In the X,Y,Z coordinates, α is given by

$$\cos\alpha=\cos\theta\cos\omega+\sin\theta\sin\omega\cos(\phi-\delta) , \tag{6}$$

where ω and δ are the angles between the polarization vector and the Z and the X axis, respectively. Since the polarization vector is in the plane of incidence and perpendicular to the sample normal, thus $\omega=90°-\theta'$ and $\delta=0°$, and Eq. (6) therefore reduces to

$$\cos\alpha=\cos\theta\sin\theta' . \tag{7}$$

(5) Repeat this procedure for different values of θ and θ' and α.

In our experiment, we took photoemission spectra by setting the analyzer at angles: $(\theta,\theta')=(60°,0°)$; $(40.2°,49.1°)$; $(50.6°,38°)$; $(0°,60°)$, with the angle α corresponding to these pairs being $\alpha=90°$, 54.7°, 67°, and 30°. The photoelectron asymmetry parameter was then simply obtained by measuring the counting rates for different values of α. According to Eq. (1), the counting rate C_1 corresponding to angle α_1 is

$$C_1(h\upsilon)=\frac{\sigma_{nl}(\varepsilon)}{4\pi}[1+\beta P_2(\cos\alpha_1)]\lambda(E_k)\xi(E_k)\Phi(h\upsilon)\cos\gamma F(\lambda,\kappa,\eta,\chi) , \tag{8}$$

and the counting rate C_2 corresponding to angle α_2 is

$$C_2(h\upsilon)=\frac{\sigma_{nl}(\varepsilon)}{4\pi}[1+\beta P_2(\cos\alpha_2)]\lambda(E_k)\xi(E_k)\Phi(h\upsilon)\cos\gamma F(\lambda,\kappa,\eta,\chi) . \tag{9}$$

The β parameter can then be determined by finding the ratio of the counting rates for different α angles, i.e.,

$$\frac{C_1}{C_2}=\frac{1+\beta P_2(\cos\alpha_1)}{1+\beta P_2(\cos\alpha_2)} . \quad (10)$$

Now calling $P_2(\cos\alpha_1)=x$ and $P_2(\cos\alpha_2)=y$, and $(C_1/C_2)=A$, we get

$$\beta=\frac{1-A}{Ay-x} . \quad (11)$$

In our experiment, we took photoemission spectra at four different α angles, and fitted the results to the form of Eq. (11). Note that many experimental uncertainties such as the electron escape depth, the photon flux intensity, the efficiency of the electron analyzer, and the light and electron reflection and refraction, which introduce a considerable amount of distortion in the measurement of the cross section do not play a role in determining the asymmetry parameter, since the β parameter is essentially determined from the ratio of the counting rates [Eq. (11)], and by using the technique described in this section, all those factors cancel out from the ratio, thus allowing an extremely accurate determination of the β parameter.

We finally wish to point out that the β parameter can also be measured by rotating the sample and the analyzer together in order to keep the angle between the sample normal and the photoelectron direction constant, while varying the angle between the polarization vector and the sample normal.[4,5] Using this technique, however, causes the angle between the sample normal and the light beam to change during the measurements. This technique, while probably adequate at energies well above the threshold where light reflection and refraction at the sample normal are rather small, is by no means applicable at energies near the threshold where light reflection and refraction are quite significant. Thus near the threshold, the only viable technique for the measurement of the β parameter is to rotate the electron analyzer in a cone around the sample normal, as described in detail in this section.

IV. RESULTS AND DISCUSSION

A. Cross section

In Fig. 3 we present experimental determinations of the Ag valence-band partial photoionization cross section at energies near the 4*d* threshold along with the theoretical calculations in the relativistic random-phase approximation (RRPA) for atomic Pd,[10] the theoretical predictions in the Herman-Skillman (HS) approximation for atomic Ag, and the experimental results for atomic Ag.[2] For graphical convenience, we have normalized our cross-section data to the RRPA results at the minimum. Ideally, we should compare our experimental data to the RRPA predictions for atomic Ag; however, the calculation for atomic Ag, which is an open shell, is more difficult and not yet available. Fortunately, the properties of the 4*d* electrons in Pd and Ag are very similar and the comparison is therefore not expected to introduce an unacceptable uncertainty. The experimental cross section for metallic Ag is very close to the experimental and theoretical results for atomic Ag and Pd, showing a slow onset in the transition strength at the threshold and then increasing monotonically with photon energy. This is in sharp contrast to the hydrogenic behavior, which is maximum at the threshold, and then starts to decrease monotonically with increasing photon energy. To understand this behavior of the cross section, we note that the σ_{4d} in the dipole approximation is essentially determined by the overlap matrix elements R_{fd} and R_{pd}, i.e.,[11]

$$\sigma_{4d}=\tfrac{8}{3}\pi^2\alpha a_0^2(\varepsilon-\varepsilon_{4d})\{2[R_{pd}(\varepsilon)]^2+3[R_{fd}(\varepsilon)]^2\} , \quad (12)$$

where ε is the energy of the ejected electron, ε_{4d} is the energy of the 4*d* electron, α is the fine structure, a_0 is the Bohr radius, and $R_{pd,fd}$ are the radial dipole matrix elements. In the energy range of interest, σ_{4d} is almost entirely determined by the characteristics of R_{fd} since $R_{fd} \gg R_{pd}$.

At the threshold, the effective potential as seen by an *f* wave electron contains a large centrifugal barrier that keeps the final state from penetrating into the atom, thus resulting in a very small overlap matrix element R_{fd} and consequently in a small cross section at the onset. With increasing the photon energy, the εf continuum penetrates the atom more effectively, thereby resulting in an increase of the overlap matrix elements and of the partial

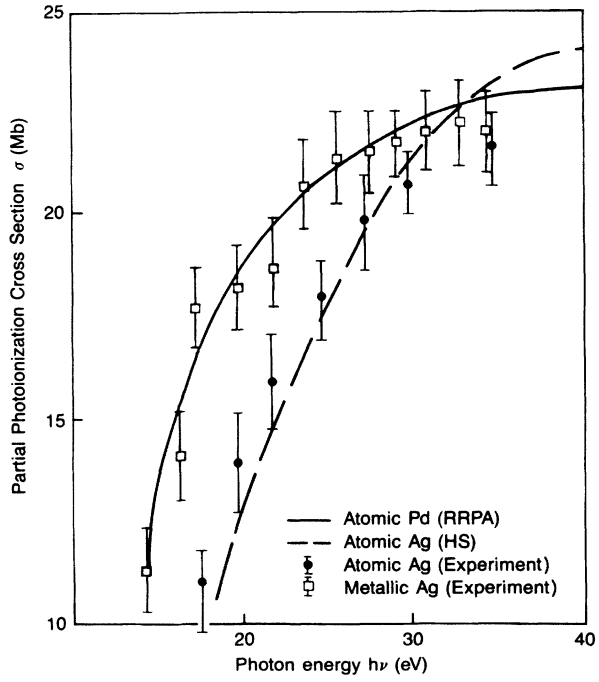

FIG. 3. The partial photoionization cross section for 4*d* electrons of Ag. Our experimental data for polycrystalline Ag (open squares) are compared with the data from atomic Ag (circle), the RRPA prediction for atomic Pd (solid line), and the HS results for atomic Ag (dashed line). Note that our experimental data are normalized at the minimum to the RRPA theoretical value.

photoionization cross section. Since the σ from metallic Ag near the threshold is very close to the atomic results, we may conclude that the repulsive term in the Hamiltonian of atomic Ag, which gives a delay in the oscillator strength, is also present in the Hamiltonian of bulk Ag.

B. Asymmetry parameter

In Fig. 4 we present experimental determinations of the 4*d* asymmetry parameter for polycrystalline Ag along with the theoretical calculations in RRPA (Ref. 10) for atomic Pd, the theoretical predictions in the HS approximation for atomic Ag, and the experimental results for atomic Ag in the photon energy range near the 4*d* threshold.[2] From the results shown in Fig. 4, the following should be noted:

(1) In the photon energy range $h\nu=14-20$ eV, the β parameter from metallic Ag shows a very small energy dependence, being almost equal to 0; however, the theoretical β parameters in the RRPA and HS approximations, in the range $h\nu=13-20$ eV, show a dramatic energy dependence, dropping rapidly from 1.3 to 0.1 and -0.4, respectively, with the β at $h\nu=14$ eV (at the onset of the measurement of the polycrystalline Ag) being almost equal to 1. The experimental β for atomic Ag, starting at around $h\nu=15$ eV, also shows a strong energy dependence, dropping from 0.5 to -0.1. Had the asymmetry of atomic Ag been carefully measured in the energy range of $h\nu=13-15$ eV, we strongly suspect that it would have dropped from 1.3 to 0.5, in close agreement with the theoretical predictions in the RRPA, since the measured β parameters of other states near the threshold agree quite favorably with the RRPA results. For example, the experimental β from Xe 4*d* shows a remarkable agreement with the theoretical calculations in the RRPA, dropping rapidly from 1.6 to 0 in the photon energy range 7 eV above the 4*d* threshold.[12]

(2) In the photon energy of 20–34 eV, our experimental asymmetry parameter data for metallic Ag are close to the atomic results, all increasing very slowly with photon energy.

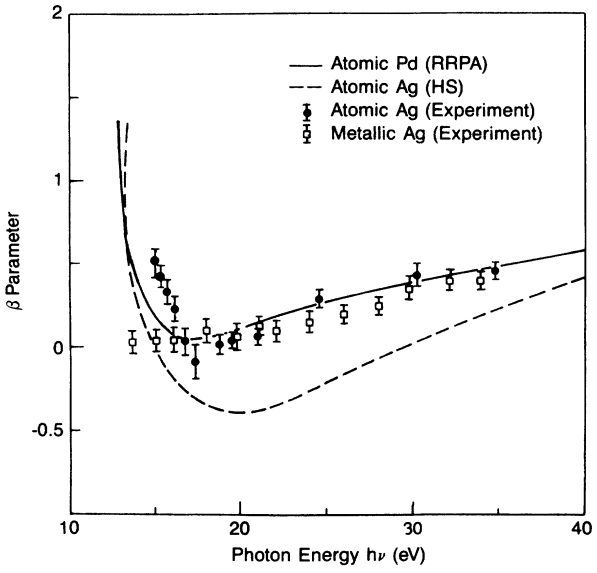

FIG. 4. The asymmetry parameter for 4*d* electrons of Ag. Our experimental data for polycrystalline Ag (open squares) are compared with the data for atomic Ag (circle), the RRPA prediction for atomic Pd (solid line), and the HS calculations for atomic Ag (dashed line).

In the following, we shall consider both atomic and solid-state effects on the β parameter. However, we believe that the solid-state effects are considerably more important than the atomic effects.

1. Atomic effects on the asymmetry parameter

We first consider atomic effects on the energy dependence of the β parameter at energies near the 4*d* threshold. To understand the results shown in Fig. 4, we note that the Ag 4*d* asymmetry parameter in the *LS* coupling and in the dipole approximation is given by:[13,14]

$$\beta(\varepsilon)=\frac{12[R_f(\varepsilon)]^2+2[R_p(\varepsilon)]^2-36R_f(\varepsilon)R_p(\varepsilon)\cos[\eta_f(\varepsilon)+\delta_f(\varepsilon)-\eta_p(\varepsilon)-\delta_p(\varepsilon)]}{15[R_f(\varepsilon)]^2+10[R_p(\varepsilon)]^2}\ , \tag{13}$$

where $\eta_{f,p}$ and $\delta_{f,p}$ are the Coulomb and the non-Coulomb phase shifts of the f and the p waves. In the photon energy range $h\nu=13-20$ eV, the strong oscillation of β is primarily due to the rapid variation of the Coulomb phase shifts, while in the energy range $h\nu=20-34$ eV, the energy dependence of β is mainly due to the variation of the non-Coulomb phase shifts.[15,16]

Since the behavior of β near the threshold is almost entirely determined by the characteristics of the phase shifts of the final-state wave function, an interpretation of the results shown in Fig. 4 requires a comparison of the asymptotic form of Ψ_f from metallic Ag to that from free atom. Obviously, the final-state wave functions for both atomic Ag and bulk Ag are solutions to the Schrödinger equation; however, the boundary conditions for the two cases are significantly different. For atomic Ag, the potential far from the origin fall off as Coulomb potential, i.e., $V(r)\rightarrow(Ze^2/r)$, and the photoelectron is never completely free, no matter how far away it gets from the origin.[17] The asymptotic form of the radial part of Ψ_f for a photoelectron leaving a Coulomb potential in the single-electron approximation can be written as[16]

$$P_{\varepsilon l}(r)\sim\sin\left[\sqrt{\varepsilon}r+\frac{1}{\sqrt{\varepsilon}}\ln 2\sqrt{\varepsilon}r-\frac{l\pi}{2}+\eta_l(\varepsilon)+\delta_l(\varepsilon)\right]\ \text{as}\ r\rightarrow\infty\ , \tag{14}$$

where the dramatic energy dependence of β for atomic Ag in the energy range 13–20 eV is caused by the rapid variation of the Coulomb phase shifts $\eta_l(\varepsilon) = \arg\Gamma(l+1-i\varepsilon^{-0.5})$ with photon energy.

For metallic Ag, however, the potential at large distances from the origin, due to the screening effects, falls off as $e^{-\kappa r}/r$. Since the potential falls faster than $1/r$, the photoelectron behaves like a free particle far from the origin, and the asymptotic form of the radial part of Ψ_f in the single-electron approximation can be written as[17]

$$P_{\varepsilon l}(r) \sim \sin\left[\sqrt{\varepsilon} r - \frac{l\pi}{2} + \delta_l(\varepsilon)\right] \quad \text{as } r \to \infty \ . \tag{15}$$

As seen in the above equation, the Coulomb phase shift, which induces the most dramatic oscillation of β in atomic Ag in the energy range $h\nu = 13$–20 eV, is absent from the final-state wave function of bulk Ag; further, the non-Coulomb phase shifts and the matrix elements are slowly varying functions of the photon energy so that they cannot cause a rapid variation in the β parameter over such a small energy range.[16,18] The absence of the Coulomb phase shifts in the final-state wave function of bulk Ag is therefore a possible explanation for the fact that its β shows a much smaller energy dependence than the free atomic case in the energy range $h\nu = 14$–20 eV.

In the photon energy range $h\nu = 20$–34 eV, the energy dependence of the asymmetry parameter is mainly due to the variation of the f wave non-Coulomb phase shifts. Because of the presence of a centrifugal barrier in the $4d \to \varepsilon f$ channel, the phase of the εf continuum increases with the photon energy, thereby causing the oscillation in the β parameter.[16] Since such a barrier is present in the Hamiltonian of both atomic Ag and polycrystalline Ag (see the discussion regarding the energy dependence of σ), the asymmetry parameter of both systems are expected to show very similar behavior, as verified experimentally.

2. *Solid-state effects on the asymmetry parameter*

We now consider solid-state effects on the behavior of the β parameter of bulk Ag at energies near the $4d$ threshold. We begin our discussion by considering the photoelectron angular distribution from the single crystalline Ag. Since the valence band of metallic Ag is approximately 3.5 eV below the Fermi level, the influence of the crystal potential on the shape of the energy band, which causes the band to distort in the vicinity of the zone edge and at other Bragg planes, should be included. In this case, Mahan has shown that the angular distribution of the photoemitted electrons is of the form,[19,20]

$$\frac{dI}{d\Omega} \sim \sum_{\mathbf{G}} (\boldsymbol{\varepsilon}\cdot\mathbf{G})^2 V_G^2 \int d^3k' \, \delta_{\mathbf{k}-\mathbf{G}-\mathbf{k}'} \ . \tag{16}$$

The δ function in the above equation indicates that the photoelectrons propagating with a wave vector $\mathbf{k}'$ are elastically scattered by the crystal potential into all other directions that are symmetrically equivalent. This is very similar to low-energy electron-diffraction (LEED) wherein a single electron beam shot at the surface produces many reflected—as well as transmitted—waves. Note that the photoelectrons measured in our experiment have energies comparable to electrons measured in LEED.

Since the effect of the crystal potential on the energy band of metallic Ag is strong, the $4d$ initial-state wave function is a Bloch wave, characterized as linear combination of plane waves. So an electron in state $\mathbf{k}'$ propagates through the crystal not only with the wave vector $\mathbf{k}'$, but also with wave vectors $\mathbf{k}'+\mathbf{G}'$ (where $\mathbf{G}'$ is a reciprocal-lattice vector). Each of these components creates an external distribution photoelectron. The primary component $e^{i\mathbf{k}'\cdot\mathbf{r}}$ creates the conic distribution of the electrons; while the other components $e^{i(\mathbf{k}'+\mathbf{G}')\cdot\mathbf{r}}$ give rise to distributions which are approximately conical and are called the secondary cones. Thus the photoelectrons emitted from the single crystalline Ag are strongly scattered into primary as well as secondary cones.

We now consider the photoelectron angular distribution from a polycrystalline sample such as polycrystalline Ag. It is well known that the evaporation of Ag onto a clean stainless-steel substrate produces crystallites with dimensions of a few hundred Angstroms, so that the band structure is certainly present in each crystallite.[21] Thus the photoelectrons emitted from each crystalline have primary and secondary conic angular distribution; for example the photoelectrons emitted from one of the crystallites have the angular distribution of the form $\sum_{\mathbf{G}} \delta_{\mathbf{k}-\mathbf{G}_1-\mathbf{k}'}$, while the electrons emitted from another crystallite (with the same energy) have the form $\sum_{\mathbf{G}'} \delta_{\mathbf{k}-\mathbf{G}_2-\mathbf{k}'}$, with $\mathbf{G}_1$ and $\mathbf{G}_2$ being randomly oriented with respect to each other. To obtain the photocurrent measured by the electron analyzer, we should add the contributions from all randomly oriented crystallites. It thus seems clear that a double randomization by scattering processes in the final states due to the periodic crystal potential and by random orientation of the crystallites leads to an isotropic photoelectron angular distribution, with the asymmetry parameter being essentially equal to zero. This is precisely the result that we observed in our experiment.

We finally want to point out that there is an interesting analogy between our photoemission experiment from polycrystalline Ag and an x-ray-diffraction experiment from a powder of randomly oriented crystallites. When a beam of nonmonochromatic x rays falls upon a crystal with a given orientation, the conditions for Bragg reflection are generally satisfied for various sets of lattice planes by particular components of the incoming beam. Each of these components is then scattered in the direction corresponding to the particular orientation of the lattice planes. The set of scattered directions form the "Laue pattern" of the crystal. When the incoming beam is monochromatic, no Laue pattern is, in general, observed for a crystal of given orientation (since the crystal is generally not oriented at the right angle to satisfy the conditions for Bragg reflection). However, if the monochromatic beam falls upon a powder of crystallites oriented at random, some of the crystallites will be oriented at the right angle for Bragg reflection on one of the various

sets of lattice planes. The scattered x rays therefore form a ring on a photographic plate, which is called the "Debye-Scherrer pattern" of the powder. Similarly in a photoemission experiment from a polycrystalline sample (such as polycrystalline Ag in our experiment), the photoemitted electrons have an isotropic angular distribution, with the β parameter being essentially zero. The analogy between x-ray diffraction and photoemission, however, is not exact because photoelectrons are scattered by individual atoms to a much greater extent than x rays.

V. CONCLUSION

We have presented the results of the first investigation of the solid-state effects on the valence-band asymmetry parameter of bulk Ag near the $4d$ threshold. We have shown that in this energy range the β from metallic Ag is dramatically deformed with respect to the free atom, and we propose that this phenomenon is primarily a consequence of a double randomization by a scattering process due to the periodic crystal potential and by random orientation of the crystallites. We finally wish to emphasize that near the threshold, the condensed-phase asymmetry parameter of all states—either core levels or valence states—are expected to be severely distorted with respect to the free atomic case, being essentially equal to zero.

ACKNOWLEDGMENTS

We wish to thank P. H. Mahowald for valuable help during the experiment. This work was supported by the National Science Foundation Materials Research Laboratory (NSF-MRL) program through the center for Materials Research at Stanford University and by the Office of Naval Research, U.S. Department of Defense, under Contract No. N00014-86-K-0736. The experiments were performed at the Stanford Synchrotron Radiation Laboratory, which is supported by the U.S. Department of Energy (Office of Basic Energy Sciences) and by the National Science Foundation (Division of Material Research).

[1]For a review, please see T. A. Carlson, M. O. Krause, W. A. Svensson, P. Gerard, F. A. Grimm, T. A. Whitely, and B. P. Pullen, Z. Phys. D **2**, 309 (1986).

[2]M. O. Krause, W. A. Svensson, T. A. Carlson, G. Leroi, D. E. Ederer, D. M. P. Holland, and A. C. Parr, J. Phys. B **18**, 4069 (1985).

[3]T. A. Carlson, A. Fahlman, M. O. Krause, T. A. Whitely, and G. A. Grimm, J. Chem. Phys. **81**, 5389 (1984).

[4]R. F. Davis, S. D. Kevan, B. C. Lu, J. G. Tobin, and D. A. Shirley, Chem. Phys. Lett. **71**, 448 (1980).

[5]M. Ardehali and I. Lindau, J. Electron Spectrosc. Relat. Phenom. **46**, 215 (1988).

[6]G. N. Kwawer, T. J. Miller, M. G. Mason, Y. Tan, Y. Ma, and F. C. Brown, Phys. Rev. B **39**, 1471 (1989).

[7]J. A. R. Samson, *Techniques of Vacuum Ultraviolet Spectroscopy* (Wiley, New York, 1967).

[8]P. W. Palmberg, J. Vac. Sci. Technol. **12**, 379 (1975).

[9]C. N. Yang, Phys. Rev. **74**, 764 (1948).

[10]V. Redojevic and W. R. Johnson, J. Phys. B **16**, 177 (1983).

[11]U. Fano and J. W. Cooper, Rev. Mod. Phys. **40**, 441 (1968).

[12]S. H. Southworth, P. H. Kobrin, C. M. Truesdale, D. Lindle, S. Owaki, and D. A. Shirley, Phys. Rev. A **24**, 2257 (1981).

[13]H. A. Bethe, in *Handbuch der Physik,* edited by H. Geiger and K. Sheel (Springer-Verlag, Berlin, 1933), Vol. 24, p. 482.

[14]J. Cooper and R. N. Zare, in *Lectures in Theoretical Physics,* edited by S. Geltman, K. Mahanthappa, and W. Brittin (Gordon and Breach, New York, 1969), Vol. II c, p. 317.

[15]S. T. Manson, Adv. Electron. Electron Phys. **44**, 1 (1977).

[16]D. J. Kennedy and S. T. Manson, Phys. Rev. A **5**, 227 (1972).

[17]See for example, *Quantum Mechanics* L. I. Schiff (McGraw-Hill, New York, 1968), p. 117.

[18]S. T. Manson, Phys. Rev. **182**, 97 (1969).

[19]G. D. Mahan, Phys. Rev. B **2**, 4334 (1970).

[20]G. D. Mahan, Phys. Rev. Lett. **24**, 1068 (1970).

[21]See for example, C. N. Berglund and W. E. Spicer, Phys. Rev. **136**, A1044 (1964).